# Dynamics and stability of 1D patterns in active polar fluids

Author: Josep-Maria Armengol Collado.
*Facultat de Física, Universitat de Barcelona, Diagonal 645, 08028 Barcelona, Spain.**

Advisor: Jaume Casademunt Viader.

**Abstract:** Turbulence in active fluids has been proposed as a new universality class of turbulence. However, the mechanisms governing these flows are poorly understood. In this work, we study numerically the formation of uni-dimensional patterns in a minimal model for an active polar nematic fluid, for arbitrary values of the flow alignment coefficient $\nu$. In addition, we determine analytically the linear stability of the asymptotic states, as a function $\nu$. We describe the complete bifurcation diagram for uniform states in 1D and show the existence of transversal (2D) instabilities, in particular in the so-called flow alignment regime $|\nu| > 1$. This result shows that the secondary instabilities leading to turbulence are not specific of the case $\nu = 0$, thus reinforcing the conclusion that active flows constitute a new universality class of turbulence.

## I. INTRODUCTION

In recent years, the nature of turbulence in active matter has become an important focus of interest in fundamental non-equilibrium physics [1]. While classical inertial turbulence is associated with large Reynolds number $Re \gg 1$, [2], a recent study [3] shows that active fluids in the Stokes limit $Re = 0$ with absence of topological defects also exhibit power-law turbulence scaling. More precisely, the kinetic energy spectrum has been shown to scale as $k^{-1}$, instead of the $k^{-5/3}$ of Kolmogorov's law, thus suggesting a new universality class of turbulence. Remarkably, the scenario of energy cascades in $k$-space is not valid for active turbulence, where energy is injected in all scales and dissipated at the same scale in which it is injected. This has only been shown in a minimal model with flow alignment coefficient $\nu = 0$, so the degree of universality of those findings is yet to be established.

Here we extend the minimal model introduced in [3] to finite $\nu$. This parameter encodes the hydrodynamic coupling between the flow $\vec{v}$ and the orientation field $\vec{p}$. As discussed in the field of liquid crystals [4], one may distinguish two qualitatively different regimes: $|\nu| < 1$, called tumbling and $|\nu| > 1$ known as flow alignment. Power-law scaling for active turbulence has been found so far for $\nu = 0$, but it has been conjectured that this behaviour should be expected for arbitrary values of the alignment coefficient. To check whether the route to turbulence observed for $\nu = 0$ is indeed generic, here we study numerically the 1D dynamical scenarios of the problem with arbitrary $\nu$, and we determine analytically the complete bifurcation diagram of uniform states, including their 2D stability, a point that is crucial to confirm the transition to chaos for arbitrary $\nu$.

The layout of this thesis is as follows. We first report the model equations that define our physical system, and we briefly report on the numerical approach developed. Then, we examine the 1D dynamics for $\nu = 0$ which yields some exact solutions. The central part of our work is the study for arbitrary values of $\nu$, in particular, focusing on the stability of stationary states in order to extrapolate consequences in 2D and confirm the route to turbulence.

*Electronic address: armengol_95@hotmail.com

## II. MODEL EQUATIONS

With the spirit of setting the simplest physical model to capture universal properties, we will take the simplest possible model of an incompressible polar nematic fluid as described in [5, 6], based solely on symmetries and linear irreversible thermodynamics. Writing the equations in dimensionless variables as described in [3] and using the stream function $\psi$, defined by $v_x = \partial_y\psi$ and $v_y = -\partial_x\psi$, it is required a long mathematical development (see [3] for details) to reach our minimal equations for $\psi$ and the angle $\theta$ of the orientation vector $\vec{p}$ (assumed to be unitary) with respect to the $x$-axis,

$$\Delta^2\psi + \frac{\rho}{2\mathcal{Z}}\Delta^2\theta + \nu\rho B(\theta) = \mathcal{S}\left(\frac{1}{2}\left(\partial_y^2 - \partial_x^2\right)\sin 2\theta + \partial_{xy}^2\cos 2\theta\right), \tag{1}$$

$$\partial_t\theta + \frac{\Delta\psi}{2} = \left(\partial_x\psi\right)\left(\partial_y\theta\right) - \left(\partial_y\psi\right)\left(\partial_x\theta\right) + \frac{\Delta\theta}{\mathcal{Z}} - \nu C(\theta), \tag{2}$$

where

$$B(\theta) = \frac{1}{2}\left(\partial_y^2 - \partial_x^2\right)\left(h_\parallel\sin 2\theta + \frac{1}{\mathcal{Z}}\cos 2\theta\Delta\theta\right) + \partial_{xy}^2\left(h_\parallel\cos 2\theta\right), \tag{3}$$

$$C(\theta) = \frac{1}{2}\cos 2\theta\left(\partial_y^2\psi - \partial_x^2\psi\right) - \sin 2\theta\partial_{xy}^2\psi. \tag{4}$$

The two dimensionless parameters are the viscosity ratio $\rho = \gamma/\eta$, being $\gamma$ and $\eta$ the rotational and shear viscosity respectively, and the activity parameter $\mathcal{Z} = |\xi\Delta\mu|\,\rho L^2/K \equiv L^2/\ell_c^2$, with $\xi\Delta\mu$ the active stress, $L$ the size of the system, $K$ the elastic

Frank constant and $\ell_c$ is an intrinsic length of the problem. Moreover, $\mathcal{S} = -\xi\Delta\mu/|\xi\Delta\mu|$ is $+1$ $(-1)$ for extensile (contractile) stresses, and finally $h_\parallel = \frac{\nu}{2}\left[\sin 2\theta\left(\partial_y^2\psi - \partial_x^2\psi\right) + \cos 2\theta\partial_{xy}^2\psi\right]$ corresponds to the parallel component of the so-called molecular field [4], the conjugate field of the polarization $\vec{p}$.

From these previous expressions, one can also compute the linear dispersion relation $\Omega(\vec{k})$ for linear perturbation of wave-vector $\vec{k}$ making an angle $\phi$ with respect to $\vec{p}$, to get a dimensionless linear growth rate $\Omega$ of the form [3],

$$\Omega(k) = -\frac{k^2}{\mathcal{Z}}\left(1 + \frac{\rho}{4}\frac{(1-\nu\cos 2\phi)^2}{1+\frac{\rho\nu^2}{8}\sin^2 2\phi}\right) + \frac{\mathcal{S}}{2}\frac{\cos 2\phi\,(1-\nu\cos 2\phi)}{1+\frac{\rho\nu^2}{8}\sin^2 2\phi}. \tag{5}$$

Due to the presence of the activity, perturbation of sufficiently long wavelength may be unstable. The growth rate is anisotropic and implies that most unstable modes occur in a 1D subspace. The outcome of the instability is thus 1D patterns, which justifies reducing the analysis on the early stages to 1D. We then fix the initial orientation of the base state to $\theta_0 = 0$ and assume, unless otherwise specified, $\partial_x = 0$.

## III. NUMERICAL APPROACH

In order to gain physical insights and to ease the way to the analytic approach, we solved the above equations in 1D using a *Matlab* code. This preliminary study was important to characterize the transient dynamics from the onset of instability to the asymptotic states at the deeply nonlinear regime, and was instrumental to guide the analytic results that will be specified later.

The usual setup for the simulations was fixing $L = 1$, and vary $\ell_c$ to address different activities. In order to have a periodic system, the perturbations considered were sinusoidal of the form $A\sin\left(k_y y + \frac{\pi}{2}\right)$, with the dimensionless amplitude $A \approx 0.75$, and the wave-vector $k_y = \frac{2\pi n}{L}$, for the different modes $n$. Then, the dynamics was solved using an Euler algorithm written from scratch. In some cases, we add a random white noise term to test the robustness of the solutions.

## IV. BEHAVIOUR FOR $\nu = 0$

In this case, not only the flow alignment coupling is neglected but also the nematic elasticity [4]. Then, it can be shown that the problem is reducible to a single dimensionless parameter that combines $\rho$ and $\mathcal{Z}$, namely $\mathcal{Z}' = \mathcal{Z}/(2+\rho/2)$ so that the dispersion relation reads

$$\Omega(k_y) = -\frac{k_y^2}{\mathcal{Z}'} - \frac{\mathcal{S}}{2}. \tag{6}$$

Then, for contractile stresses, the system will always be unstable under perturbations of $k_y < k_{crit} \equiv \sqrt{\mathcal{Z}'} = L/\ell_c'$. It is important to highlight that, contrary to the common scenario in non-equilibrium pattern formation, here there is not a natural selection of an intrinsic wavelength at linear level, since the evolution will be dominated by the perturbation with lowest $k_y$, limited by the system size. On the other hand, the equation that governs the dynamics is simplified to the Overdamped Sine-Gordon equation

$$\partial_t\theta = \frac{1}{2\mathcal{Z}'}\partial_y^2\theta + \frac{1}{4}\sin 2\theta = -\frac{1}{2}\frac{\delta\mathcal{L}\left[\theta\left(y'\right)\right]}{\delta\theta\left(y\right)}, \tag{7}$$

$$\mathcal{L}\left[\theta\left(y'\right)\right] = \frac{1}{2}\int dy'\left(\frac{1}{\mathcal{Z}'}\left(\partial_{y'}\theta\right)^2 - \sin^2 2\theta\right), \tag{8}$$

being $\mathcal{L}$ a Lyapunov functional, i.e., a non-equilibrium potential that has to be minimized and relaxes the evolution until a stationary state. In fact, these can be found by identifying the expression with the nonlinear pendulum equation (writing time and angle instead of $y$ and $2\theta$), so the solutions span wavelengths between $\lambda = 2\pi\ell_c'$ with small amplitude and infinite wavelength, with domains connected by the kink function (assuming that $\theta(-\infty) = -\pi/2$ and $\theta(\infty) = \pi/2$) given by

$$\theta_{kink} = \pm\tan^{-1}\left[\exp\left(\sqrt{\mathcal{Z}'}\left(y - y'\right)\right)\right] \mp \frac{\pi}{2}. \tag{9}$$

For large systems ($L \ll \ell_c'$), the relaxational dynamics given by Eq. (7) will produce a coarsening dynamics until a periodic state of wavelength $L$ is reached, where states of uniform angle are connected by such kink-antikink solutions.

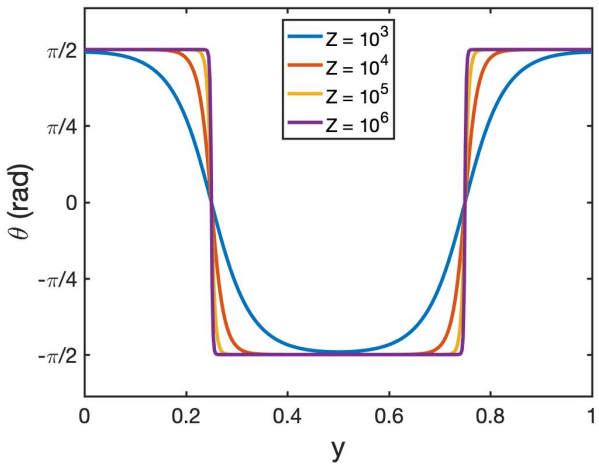


FIG. 1: Orientation field in the asymptotic stationary states for $\nu = 0$ and different values of the activity parameter $\mathcal{Z}$, with a fixed $\rho = 1$.

The width of the step between the asymptotic values is of the order of $\ell_c'$, so for $\mathcal{Z}' \gg 1$, the states with uniform angle $\pm\frac{\pi}{2}$ will be separated by very narrow walls splitting

the original system into two domains perpendicularly orientated respect to the original angle but with opposite sense of rotation. Note also that the $x$-component of the velocity is localized at the transition regions between the saturation angles, while the fluid is at rest in the regions of uniform angle.

Remarkably, the same instability of a uniform polarization will apply now in the 2D system, under perturbations in the $x$-direction. This induces a transient cascade of instabilities into smaller length scales that will only cease at scales of the order of $\ell_c'$.

## V. BEHAVIOUR FOR $\nu \neq 0$

As we will examine now, the fact of not neglecting elastic contributions makes the system much richer. From Eq. (1), (2), and considering a $x$-homogeneous fluid, we obtain the 1D dynamical equation of the form

$$\partial_t\theta = \left[\frac{4+\rho\left(\nu^2+1\right)+2\rho\nu\cos 2\theta}{\mathcal{Z}\left(4+\nu^2\rho\sin^2 2\theta\right)}\right]\partial_y^2\theta - \mathcal{S}\sin 2\theta\frac{1+\nu\cos 2\theta}{4+\nu^2\rho\sin^2 2\theta}. \quad (10)$$

Here we will not address variations of $\rho$. First of all, note that this expression does not admit any reduction of their variables $\rho$, $\mathcal{Z}$, and to our knowledge it is studied for the first time. Its stationary states will be given by

$$\frac{\left[4+\rho(\nu^2+1)+2\rho\nu\cos 2\theta\right]\partial_y^2\theta}{\mathcal{Z}} = -\sin 2\theta\left(1+\nu\cos 2\theta\right). \quad (11)$$

This cannot be solved analytically, but contains similar kink-antikink solutions, with widths fixed by the prefactor of $\partial_y^2\theta$ and connecting uniform asymptotic angles given by the zeroes of the right-hand side. Accordingly, the stationary uniform angle $\theta_{stat}$ of solutions reached (locally) at long times will be given by $\sin 2\theta_{stat}\left(1+\nu\cos 2\theta_{stat}\right)=0$, that is,

$$\theta_{stat}^{(1)}=0, \quad \theta_{stat}^{(2)}=\pm\frac{\pi}{2}, \quad \cos\left(2\theta_{stat}^{(3)}\right)=-\frac{1}{\nu}. \quad (12)$$

Note that the two values of $\theta_{stat}^{(2)}$ correspond to the same state, given the nematic symmetry of the problem. Notice also that the three possibilities are stationary solutions only when $|\nu|>1$, while for tumbling regimes ($|\nu|<1$) only $\theta_{stat}^{(1)}$ and $\theta_{stat}^{(2)}$ are achievable. Moreover, when $\nu>1$ we have $|\theta_{stat}^{(3)}|\in\left(\frac{\pi}{4},\frac{\pi}{2}\right)$ but for $\nu<-1$, the range is $|\theta_{stat}^{(3)}|\in\left(0,\frac{\pi}{4}\right)$ instead. All of these results are actually supported by numerical simulations that reflect the same situation as explained in the previous section: a coarse-graining dynamics of small perturbations towards an stationary kink-antikink solution with $\theta_{stat}^{(1)}$, $\theta_{stat}^{(2)}$ and $\theta_{stat}^{(3)}$ as the asymptotic values for the orientation field. However, there are two notable differences. On the one hand, the $x$-component of the velocity does not vanish but shows a constant shear, which can be analytically derived from Eq. (1) to obtain

$$\partial_y^2\psi=\partial_y v_x=\frac{2\mathcal{S}\sin(2\theta)-2\rho\mathcal{Z}^{-1}\partial_y^2\theta\left(1+\nu\cos(2\theta)\right)}{4+\rho\nu^2\sin^2(2\theta)}. \quad (13)$$

Hence, in the saturation regions of $\theta_{stat}^{(1)}$ and $\theta_{stat}^{(2)}$ the situation is the same discussed before for $\nu=0$, but the new stationary orientation is qualitatively different, involving a constant gradient of velocities. The extreme values of $v_x$ are achieved in the transition kink regions, specifically at the points where $\theta$ vanishes. The other special feature is that the stationary angle achieved depends on the flow alignment coefficient (see the illustration of this discussion in FIG. 2 and FIG. 3). To fully understand what are the actual asymptotic values of the angle selected by the dynamics one requires to determine their linear stability.

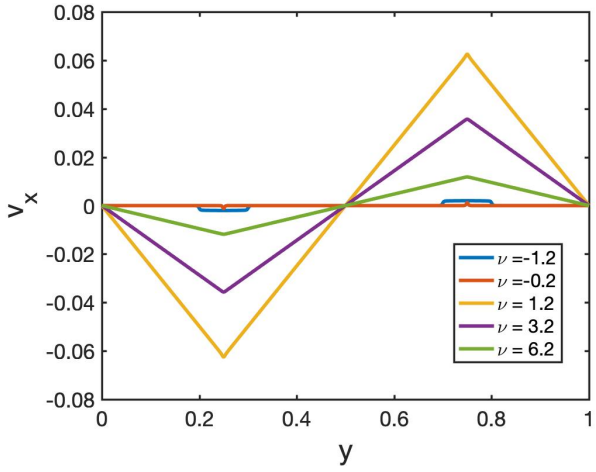


FIG. 2: Dimensionless $x$-component of the velocity of the stationary state of the system for several values of the alignment coefficient, with $\mathcal{Z}=10^6$ and $\rho=1$.

### A. 1D linear stability of stationary solutions

To explain which stationary angles will be selected by the 1D dynamics for a given flow alignment coefficient $\nu$ we address the linear stability analysis of uniform angle solutions. The 1D version of Eq. (5) for the corresponding perturbations in $y$ ($\partial_x=0$ or $\phi=\pm\frac{\pi}{2}$) is

$$\Omega(k_y)=-\frac{k_y^2}{\mathcal{Z}}\left[1+\frac{\rho}{4}(1+\nu)^2\right]-\frac{S}{2}(1+\nu). \quad (14)$$

We see that for contractile stresses ($S=-1$), the system will be unstable whenever $\nu>-1$, and so, $\theta_{stat}^{(1)}$ will be stable only when $\nu<-1$. The case of $\theta_{stat}^{(2)}$ is symmetrically equivalent to the case of a $k_x$-perturbation ($\phi=0$)

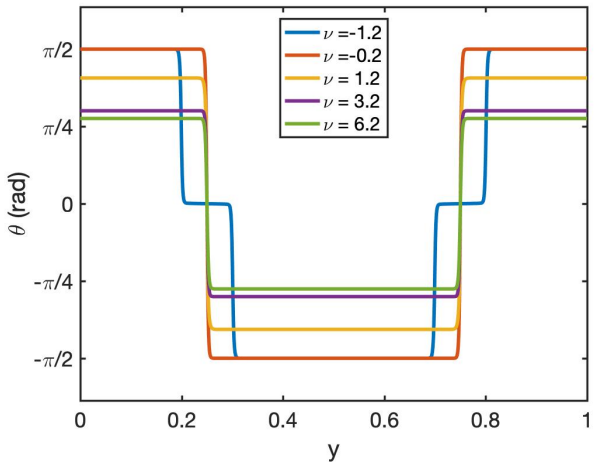


FIG. 3: Asymptotic stationary states for the orientation for different values of $\nu$ when $\mathcal{Z} = 10^6$ and $\rho = 1$.

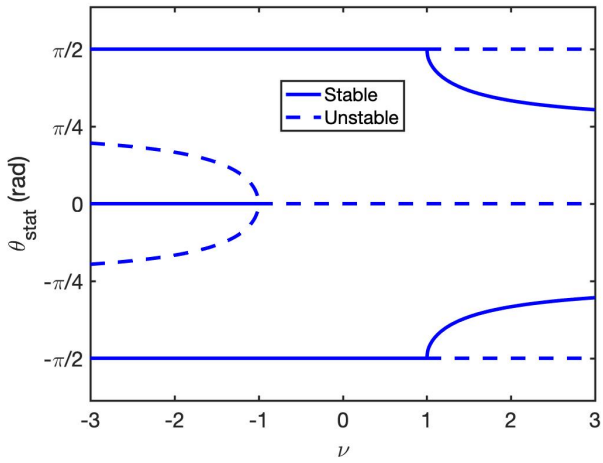


FIG. 4: Exact bifurcation diagram for solutions with uniform angle as a function of $\nu$, including their linear stability within the 1D dynamics.

to the initial state $\theta_0 = 0$, so we will have

$$\Omega(k_y) = -\frac{k_y^2}{\mathcal{Z}}\left[1 + \frac{\rho}{4}(1-\nu)^2\right] + \frac{S}{2}(1-\nu), \qquad (15)$$

Then, this case will be stable when $\nu < 1$ (assuming $\mathcal{S} = -1$). Finally, for $\theta^{(3)}_{stat}$, we have to perform the linear stability analysis anew, since the constant shear makes this state not directly reducible to Eq. (5). We have made this analysis taking into account that at this time the perturbation affects states with $\vec{v} \neq 0$ given by Eq. (13) when $\theta = \theta^{(3)}_{stat}$. Let us define $A(\nu) \equiv \partial_y v_x$ by the right-hand side of Eq. (13). After some algebra, we deduce that the linear growth rate takes the form,

$$\Omega(k_y) = -\frac{k_y^2}{\mathcal{Z}} - |A(\nu)|\,\nu\sqrt{1 - \frac{1}{\nu^2}}. \qquad (16)$$

Notice that this relation is independent of $\mathcal{S}$. Now, a careful analysis of all possible cases including different signs of the alignment coefficient conclude that the states $\theta^{(3)}_{stat}$ are only linearly stable for $\nu > 1$.

We can summarize all possible cases in a bifurcation diagram (FIG. 4) that describes all branches of possible stationary solutions and their stability together in the same plot. From there, we observe the existence of two pitchfork bifurcations at $\nu = \pm 1$ that control the dynamic evolution in the whole range of $\nu$.

Correspondingly, we can also plot in FIG. 5 the gradient of $v_x$ as a function of the alignment coefficient of the stationary cases, which must follow Eq. (13). From there, we observe that it presents a maximum (minimum) for negative (positive) values of $\theta^{(3)}_{stat}$. We can derive its exact expression which reads

$$\nu_m = \pm\sqrt{\frac{3\rho + \sqrt{\rho(\rho+32)}}{4\rho}}. \qquad (17)$$

In fact, we are interested in the positive sign since the negative one corresponds to the unstable solution. This is a decreasing function of the viscosity ratio, so the lower $\rho$, the bigger (in modulus) this extreme value will be.

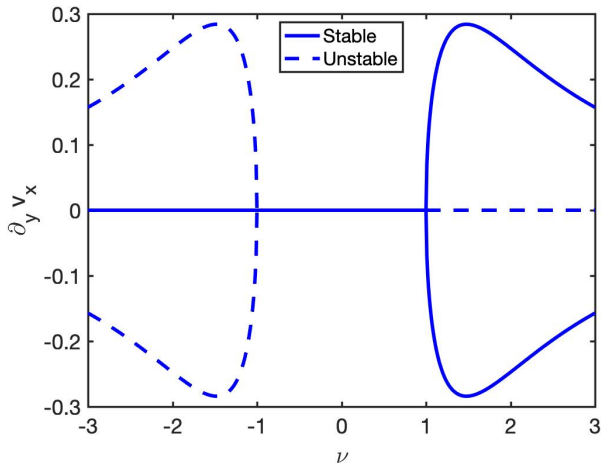


FIG. 5: Dimensionless stationary shear rate as a function of $\nu$, for the stationary solutions with uniform angle, showing also the 1D linear stability of the corresponding states. It was taken $\rho = 1$.

### B. 2D linear stability of stationary solutions

In line with the reasoning for $\nu = 0$, we try to infer consequences on the two-dimensional dynamics by studying the stability of the 1D patterns, with large domains of uniform angle, now to transversal $k_x$-perturbations.

For the situation at hand of $\mathcal{S} = -1$, let us distinguish cases according to the saturation angle achieved.

Beginning with the stable stationary $\theta^{(1)}_{stat}$, the solution obtained when $\nu < -1$, we can recover the result for a $k_x$-perturbation from Eq. (15) exchanging $x$ by $y$, and consequently, this state will be stable to this perturbation. For $\theta^{(2)}_{stat}$ (obtained only when $\nu < 1$), we repeat the symmetry discussion to take advantage of Eq. (14) and deduce that it will also be $k_x$-unstable if $\nu > -1$, giving rise to the cascade phenomena discussed in the previous section for $\nu = 0$. Finally, to test the stability of $\theta^{(3)}_{stat}$, a new development is required. We use an ansatz of the form $\theta = \theta^{(3)}_{stat} + \delta\theta$, $\psi = \psi^{(3)}_{stat} + \delta\psi$, with $\delta\theta = \theta^{(3)}_{stat} e^{ik_x x + \Omega t}$ and $\delta\psi = \psi^{(3)}_{stat} e^{ik_x x + \Omega t}$ the transverse perturbation respect to the equilibrium state $\cos(2\theta^{(3)}_{stat}) = -\frac{1}{\nu}$, $\partial_y^2 \psi^{(3)}_{stat} = A(\nu)$, which is constant for a given $\nu$. After a long calculation that we cannot include here, we obtain the following notable result,

$$\Omega\left(k_x\right) = -\frac{k_x^2}{\mathcal{Z}}\left[1 + \frac{4\rho}{4 + \rho\left(\nu^2 - 1\right)}\right] - \frac{4S}{\nu\left[4 + \rho\left(\nu^2 - 1\right)\right]}, \tag{18}$$

implying that the nontrivial branch of states with intermediate $\nu-$dependent angles for $\nu > 1$ will always be $k_x$-unstable. Furthermore, note that the most unstable perturbation will be given when $\nu = 1$, implying a maximum linear growth rate of value 1.

To sum up, all stationary stable states for $\nu > -1$ resulting of perturbations along $y$-axis turn up to be unstable for perturbations in the perpendicular $x$-direction. Accordingly, the physical picture of 1D coarse-graining dynamics followed by secondary instabilities in the transversal direction identified as a route to turbulence in [3] can be extrapolated to the complete tumbling regime, and most importantly to the alignment regime ($\nu > 1$ for $S = -1$ and $\nu < -1$ for $S = +1$, the latter not shown), a case which is qualitatively different because of the structure of the flow field. These results reinforce the claim of universality for the transition to turbulence in active fluids.

## VI. CONCLUSIONS

We have studied analytically and numerically the early stages of the instability of a uniformly oriented active polar nematic fluid, which is dominated by the one-dimensional dynamics. The aim was to extend the scenario of transition to active turbulence elucidated for $\nu = 0$, to arbitrary values of this parameter, in order to explore the universality of the phenomenon. The specific tasks and results are the following:

- We have developed a *Matlab* code for general 1D dynamics of the problem, allowing for a detailed study of the coarse-graining evolution. We have obtained numerically the steady states including the kink solutions and the structure of the flow field in the fully nonlinear regime.

- In the tumbling regime ($|\nu| < 1$), we have extended the results of $\nu = 0$ to domains with angle $\pm\frac{\pi}{2}$ and vanishing velocity, confirming also their instability to transversal 2D perturbations.

- In the flow alignment regime ($|\nu| > 1$), we must distinguish between positive and negative values of $\nu$. When $\nu < -1$, the stable stationary angles are $0, \pm\frac{\pi}{2}$ which remain also stable in 2D. On the contrary, for $\nu > 1$, new branches of stable uniform orientation states are found at $\pm\frac{1}{2}\arccos\left(-\frac{1}{\nu}\right)$, with nontrivial constant shear flow. Most importantly, we have found that these are also unstable to transverse 2D perturbations. This result reinforces the claim of universality of the transition to turbulence in active fluids.

To conclude, it is worth mentioning the natural outlook of this work into the pursuit of the study for the full 2D dynamics, to characterize the turbulence not only with a scaling exponent but also by quantifying its effective embedding dimension. The main objective would be to certify that chaotic active flows do constitute a new universality class of turbulence.

### Acknowledgments

I would like to express my gratitude to my advisor Dr. Jaume Casademunt for his constant help, advice and conveying me his enthusiasm for physics. I also want to thank my parents and friends for his encouragement during this period of my life.

[1] L. Giomi, "Geometry and Topology of Turbulence in Active Nematics". Physical Review X **5**: 1-11 (2015).

[2] A. N. Kolmogorov, "The Local Structure of Turbulence in Incompressible Viscous Fluid for Very Large Reynolds Numbers". Proc. of the Royal Society A: Mathematical, Physical and Eng. Sciences **434**, No. 1890: 9-13 (1991).

[3] R. Alert, J. F. Joanny, J. Casademunt, "Universal scaling of defect-free active turbulence". [Unpublished].

[4] P.G. de Gennes, J. Prost, *The Physics of Liquid Crystals*, 2nd. ed. (Oxford Science Publications, 1993).

[5] M. C. Marchetti, J.F. Joanny, S. Ramaswamy, T.B. Liverpool, J. Prost, M. Rao, R. A. Simha, "Hydrodynamics of soft active matter". Reviews of Modern Phyics **85**: 1143-1189 (2013).

[6] R. Voituriez, J.F. Joanny, J. Prost, "Spontaneous flow transition in active polar gels". Europhysics Letters **70**, No. 3 (2005).